Optics Letters

Interlocking Kerr-microresonator frequency combs for microwave to optical synthesis

Travis C. Briles,[1,2,*] Jordan R. Stone,[1,2] Tara E. Drake,[1] Daryl T. Spencer,[1] Connor Fredrick,[1,2] Qing Li,[3] Daron Westly,[3] B. R. Ilic,[3] Kartik Srinivasan,[3] Scott A. Diddams,[1,2] and Scott B. Papp[1,2]

[1]Time and Frequency Division, National Institute of Standards and Technology, Boulder, Colorado 80305, USA
[2]Department of Physics, University of Colorado, Boulder, Colorado 80309, USA
[3]Center for Nanoscale Science and Technology, National Institute of Standards and Technology, Gaithersburg, Maryland 20899, USA
*Corresponding author: travis.briles@nist.gov

Received 23 February 2018; revised 4 May 2018; accepted 8 May 2018; posted 9 May 2018 (Doc. ID 324666); published 14 June 2018

We report accurate phase stabilization of an interlocking pair of Kerr-microresonator frequency combs. The two combs, one based on silicon nitride and one on silica, feature nearly harmonic repetition frequencies and can be generated with one laser. The silicon-nitride comb supports an ultrafast-laser regime with three-optical-cycle, 1-picosecond-period soliton pulses and a total dispersive-wave-enhanced bandwidth of 170 THz, while providing a stable phase-link between optical and microwave frequencies. We demonstrate nanofabrication control of the silicon-nitride comb's carrier-envelope offset frequency and spectral profile. The phase-locked combs coherently reproduce their clock with a fractional precision of $<6\times10^{-13}/\tau$, a behavior we verified through 2 h of measurement to reach $<3\times10^{-16}$. Our work establishes Kerr combs as a viable technology for applications like optical-atomic timekeeping and optical synchronization.

OCIS codes: (140.3948) Microcavity devices; (190.4390) Nonlinear optics, integrated optics.

https://doi.org/10.1364/OL.43.002933

The invention of optical-frequency combs opened many new applications [1] in photonics from precision timing and ranging to generation of entangled states [2]. They are composed of hundreds to millions of optical modes whose frequencies conform to a simple relationship, $\nu_n = n\times f_{\mathrm{rep}} + f_0$, where n is the mode number, f_{rep} is the repetition frequency, and f_0 is the carrier-envelope-phase offset frequency. Phase locking f_{rep} and f_0 delivers to users a fully stabilized frequency comb, which can be derived from the SI second.

Recently, investigations of Kerr microresonators have led to advances in parametric-optics comb generation [3], particularly in ultrahigh-speed optical waveforms [4,5] and photonic-chip integration [6]. Dissipative-Kerr soliton (DKS) pulses that stably propagate in Kerr microresonators [7,8] are thus far the most useful localized nonlinear pattern of the electromagnetic field. There have been several advances in the field, including development of various resonator materials [6,9,10], demonstrations of visible [11] mid-infrared [12] and octave-spanning operation [13,14], chip-based optical clocks [15], and studies on DKS crystallization [16]. DKS combs have also been developed for the goal of 2f-3f and f-2f self-referencing with external spectral broadening for counting optical cycles [17], carrier-offset frequency control [18], and optical-clock comparisons [19], and for 2f-3f measurements with a photonic-chip-integrated soliton comb [20,21]. Kerr combs with f_0 stabilization open capabilities like optical-frequency synthesis [22] and SI stabilization for the applications mentioned previously.

In this work, we explore a Kerr-frequency-comb system built around f_0 phase stabilization. We draw on notable strengths of Kerr-soliton combs—low noise, a wide design space, and chip integration. Our interlocked configuration of one silica and one silicon-nitride (Si_3N_4 and hereafter SiN) resonator leverages both nanofabrication and photonic-chip integration. Operating the silica Kerr comb at a microwave rate provides a dense but narrow-bandwidth reference grid, while the terahertz-rate SiN comb provides more than an octave of bandwidth for f-2f self-referencing. The key to f_0 stabilization is design and control of the ultrafast pulse circulating in the SiN resonator, including its multiple quasi-CW dispersive waves (DWs) and the magnitude of f_0 that can vary practically to 0.5 THz. We show that such a complex soliton Kerr comb permits low-noise phase stabilization of its repetition and offset frequencies with respect to the SI second, and we verify its accuracy and precision to better than 3×10^{-16} through out-of-loop measurements with an auxiliary self-referenced comb.

Figure 1 presents an overview of our experiment and key results, and the subsequent figures present analysis of the system. We implement an interlocked, dual-microresonator Kerr comb [Fig. 1(a)], which is designed principally for photonic-chip integration and low-power consumption. When interlocked with the silica comb, the SiN comb mode frequencies are $\nu_n = n\times f_{\mathrm{wide}} + f_0 = n(Hf_{\mathrm{fine}} + f_{\mathrm{rem}}) + f_0$, where f_{wide} (f_{fine}) is the repetition frequency of the SiN (silica) comb, and H and f_{rem} are the integer part and remainder of the ratio $f_{\mathrm{wide}}/f_{\mathrm{fine}}$, respectively. The silica chip contains a wedge resonator with 21.97 GHz free spectral range that has been described elsewhere [10], and we use a tapered fiber to couple

50 mW to the device. Recent work on silica resonators with integrated waveguide couplers [23] will eliminate the tapered fiber in future work. Alternatively, a SiN resonator with internal $Q = 10^7$ could operate at $f_{\text{fine}} = 25$ GHz with 25 mW of on-chip power. The SiN resonator is surrounded by a photonic circuit with two integrated couplers for efficient extraction of the >180 THz comb bandwidth. The through port is optimized for wavelengths between 1 and 1.8 μm, and the drop port is optimized for >2 μm. Currently, the SiN comb is operated with 200 mW of on-chip power, but we note that improving the internal Q to $\sim 4 \times 10^6$ will reduce required on-chip power to <25 mW, which is compatible with many integrated lasers. The threshold powers in the bus for parametric oscillation are 10 and 16 mW for the silica and SiN resonators, respectively. Figure 1(b) presents a scanning electron microscope (SEM) image of the SiN chip with annotations indicating the couplers' role.

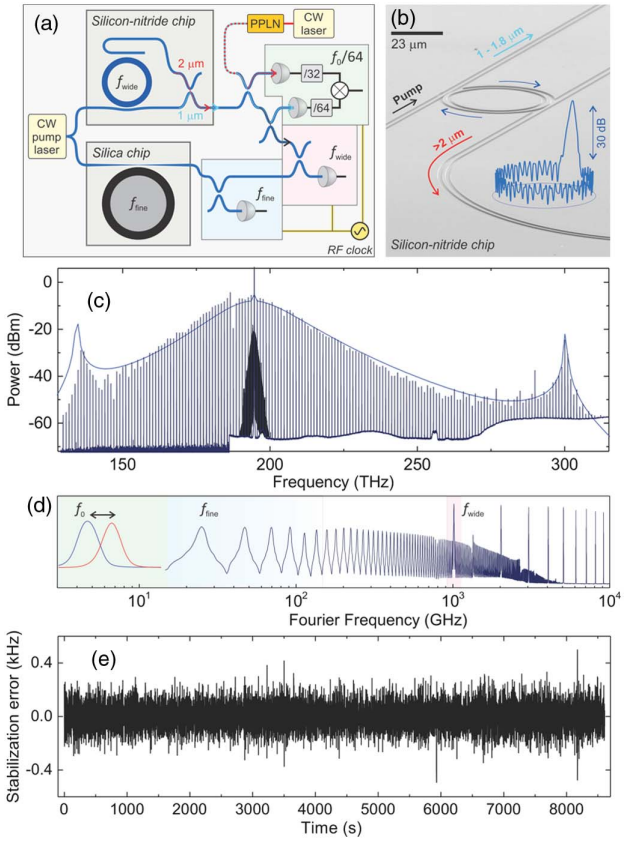

Fig. 1. Interlocked Kerr comb for absolute f_0 stabilization. (a) System diagram indicating the microresonators, photonics, detection electronics, and RF clock for stabilization. Electro-optic frequency shifters between pump laser and resonators, FS 1 and FS 2, are not shown. Frequency mixing as indicated yields f_0 in our experiments. (b) SEM image of the SiN chip with add/drop coupler configuration. (c) Optical spectrum of the two-soliton comb. The 1-THz-spaced modes are easily resolved, and the silica comb modes could be seen by expanding the plot between 190 THz and 200 THz. (d) Conceptual hierarchy of our interlocked comb scheme, exploiting stepwise upconversion of an input RF clock. The highlighted frequency ranges indicate electronically detectable f_0, and fine and wide repetition frequencies, f_{fine} and f_{wide}, respectively. (e) Absolute optical stabilization error of the interlocked Kerr combs, evaluated by comparison to an auxiliary self-referenced erbium-fiber frequency comb.

Operationally, we generate DKS pulses in both microresonators by controlling their pump frequencies independently with single sideband frequency shifters, FS 1 and FS 2. A standard external-cavity diode laser provides sufficient performance for all our experiments. These frequency shifters provide 5 GHz of sweep range and <100 ns sweep speed to counter thermal effects in the microresonators [24,25]. An optical spectrum of the interlocked soliton comb is shown in Fig. 1(c). The finely spaced silica comb covers the telecom C-band, and the SiN comb with corresponding sech^2 DKS duration of three optical cycles extends over more than 170 THz across the near IR, including its two DW components at 300 THz (999 nm) and 137 THz (2191 nm) that arise from higher-order corrections to the group-velocity dispersion [13,20,26]. The blue trace results from a simulation of a nonlinear Schrödinger equation, known as the Lugiatio–Lefever equation (LLE) [8] that mostly captures the spectral envelope of the SiN soliton comb through our measurements of Q and pump power, and finite-element modeling (FEM) of the device mode frequencies. The small discrepancies between the observed and simulated spectra are attributed to a ~5 nm fabrication tolerance in resonator dimensions and residual wavelength-dependent absorption in the SiN material. The corresponding LLE intracavity intensity is inset to Fig. 1(b) and shows the DKS propagating atop the CW pump background and the dispersive waves.

The goal of our work is to electronically phase lock the three degrees of freedom (f_0, f_{wide}, f_{fine}) that define the ν_n mode spectrum of the combs. To understand their relationships, Fig. 1(d) presents a Fourier view of the frequency combs that would notionally be created by photodetection of the comb after second-harmonic generation for f-2f self-referencing. This plot highlights how all the optical comb modes—and the 12 GHz f_0 frequency of the wide comb—are resolved by a moderate resolution spectrometer. Activating phase-locked loops for (f_0, f_{wide}, f_{fine}) with respect to a hydrogen-maser RF clock fully stabilizes the combs. We perform an out-of-loop verification of the interlocked Kerr comb using an auxiliary reference comb, which is also stabilized to the RF clock. Figure 1(e) shows a nearly 9000 s frequency-counter record of the optical heterodyne beat between the two combs, indicating their relative statistical fluctuations of 117 Hz in a 1 s observation window and mean difference of -0.052 ± 0.057 Hz on the 194.635,926,272,000 THz carrier frequency. Longer measurements should be possible with improvements to laboratory thermal and acoustic stability.

Our experiments require not only DKS generation in the SiN device, but formation of intense dispersive waves to aid f-2f interferometry, and adjustment of f_0 to less than ~20 GHz for practical photodetection. We adjust f_0, the soliton bandwidth, and the dispersive-wave spectral peaks by optimizing the geometry of the SiN ring. The ring radius (RR) and the ring-waveguide width (RW) are varied in the nanofabrication process through different device instances on the same chip. Figures 2(a) and 2(b) present an investigation into how three discrete 12.5 nm adjustments to RW with RR fixed at 23.0 μm affect the Kerr-soliton comb f_0 frequency and DW wavelengths, respectively. In particular, the carrier-envelope-offset frequency is $f_0 = \nu_p - M f_{\text{wide}}$, where M is the mode number of the pump mode in our experiments. We characterize f_0 at the MHz level with a wavemeter measurement of ν_p and knowledge of f_{wide}, which depends sensitively on RW

and RR, and on the mode number of the pumped resonance, due to the higher order group-velocity dispersion. These behaviors are captured in Fig. 2(a) in which the RW is varied, and we measure f_0 for three adjacent modes at 1540, 1548, and 1556 nm for RW = 1787.5 nm. Agreement with FEM simulations of the SiN TE1 mode frequencies (black lines) is critical in closing the loop between design, nanofabrication, and operation of comb systems. Our present analysis requires a correction of only ~5 nm to the SiN dimensions used in the FEM analysis. The soliton bandwidth and DW wavelengths also vary significantly with RW [Fig. 2(b)], and this is critical for matching the Kerr-comb spectrum to applications. The FEM results [Fig. 2(b)] are accurate enough that a sweep of a few SiN rings on a single chip can yield the desired spectral coverage.

With the interlocked Kerr combs of Fig. 1(c), we focus on their phase stabilization with respect to the RF clock. Due to off-chip coupling losses, somewhat insufficient SiN comb line powers, and the second-harmonic generation (SHG) efficiency of available periodically-poled lithium niobate (PPLN) devices at 150 THz (1998 nm), we utilize an auxiliary CW laser operating near the THz comb tooth at 150 THz. The relative detuning between the SiN comb and SHG of the CW laser at 150 and 300 THz, respectively, is monitored with optical-heterodyne signals, which are electronically processed to generate a single RF tone that is exactly $f_0/64$ and subsequently stabilized in a phase-locked loop [green box of Fig. 1(a)]. The silica comb repetition frequency is photodetected [blue box of Fig. 1(a)]. The SiN comb repetition frequency is given by $f_{\text{wide}} = Hf_{\text{fine}} + f_{\text{rem}}$. f_{rem} is measured by taking a heterodyne between the two combs, which is then electronically processed with the 46th harmonic of f_{fine} to determine f_{wide} [red box of Fig. 1(a)]. To stabilize these three signals, we search for the optimum electronic feedback pathways to the combs, which we currently understand to be pump laser power for f_0 and the settings of FS 1 and FS 2 for f_{wide} and f_{fine}, respectively. Digital phase locks are applied simultaneously.

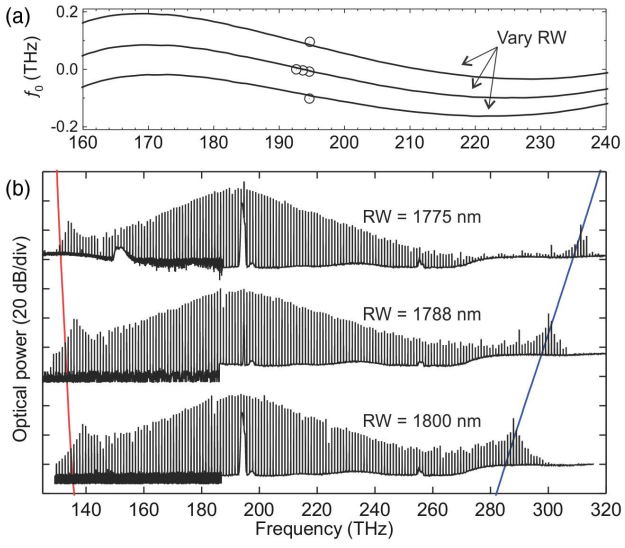

Fig. 2. (a) and (b) Design and control of f_0 and the SiN soliton bandwidth through the device RW. Curves in (a) are ordered as in (b). The solid red and blue lines track the expected locations of the dispersive waves from the LLE simulation. The pump laser has been numerically removed from each spectrum for compact display of the data.

The wide and fine comb repetition frequencies feature prominent signals at the lock points, while f_0 following digital division by 64 is coherently locked to its RF reference.

We characterize the residual-noise contribution of the phase locks, which is additive with RF-clock noise, to understand the absolute frequency stability of the interlocked comb modes. We record the phase-locked signals with a continuous Π-type frequency counter, which we convert to Allan deviation, and with an electronic spectrum analyzer. We estimate $4 \times 10^{-14}/\tau$ is the residual noise added by imperfect feedback loops by addition of the variances of the in-loop noise shown in Fig. 3(b). No more than 2 Hz of noise is contributed to the optical modes in a 1-s acquisition time, and the contribution is less with longer acquisitions due to the relative coherence to the RF clock that also gates the frequency counter.

Complete phase stabilization of our interlocked Kerr comb generates an accurate and precise set of comb mode frequencies ν_n with respect to the RF setpoints of f_{fine}, f_{wide}, and f_0, which are all derived from the RF clock. For verification, we divert a fraction of the SiN comb output for frequency measurements via optical heterodyne beats with an auxiliary self-referenced erbium-fiber optical frequency comb [27] that is referenced to the RF clock. The result is a frequency-counter record of the pump laser SiN mode ($n = 192$) at 194 THz [Fig. 1(e)] that we analyze with the overlapping Allan deviation [Fig. 3(a)]. We obtain similar data and conclusions for the $n = (189, 190, 191, 193)$ SiN comb modes, and we can infer the stability of all the comb modes, since f-2f locking stabilizes the entire comb span. The absolute fractional-frequency stability of the synthesized comb is $6 \times 10^{-13}/\tau$, where τ indicates

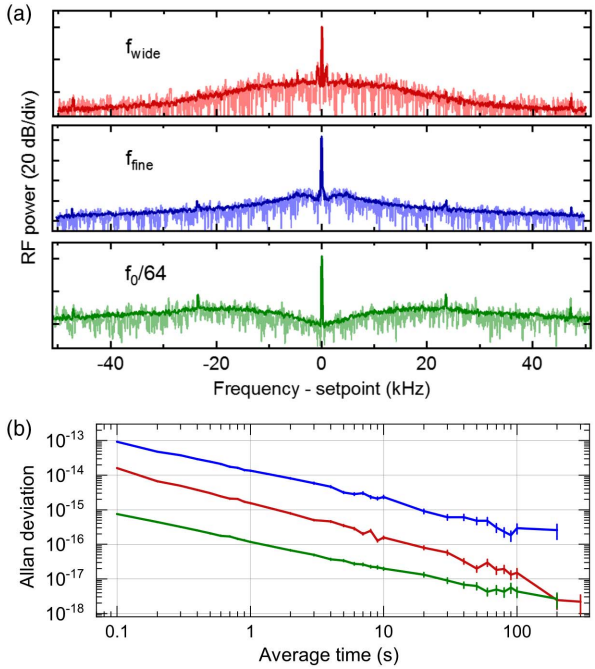

Fig. 3. Phase stabilization of the interlocked Kerr combs. (a) Power-spectral density of the carrier-envelope-offset frequency (green), the silica comb repetition frequency (blue), and the SiN comb repetition frequency (red). Each panel displays single acquisition (lighter shade) as well as a trace with 25 avgs (darker shade). (b) Residual-frequency-noise contribution of the phase locks. Frequency counter gate time is 0.1 s and normalization is to the carrier frequency of the signals.

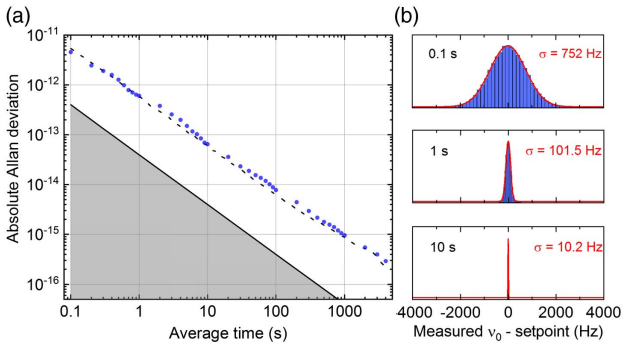

Fig. 4. Stability and accuracy of the $n = 192$ SiN comb mode. (a) Overlapping Allan deviation (blue circles) measured with the auxiliary comb by heterodyne beats with >30 dB SNR, and total contribution from microwave synthesizers (dashed line). The gray shaded region indicates the residual noise of the Kerr-comb phase locks. (b) Histogram of frequency counter (0.1 s gate time) record used to obtain the overlapping Allan deviation for 0.1, 1, and 10 s acquisitions.

the observed linear dependence with average time. This behavior confirms the stable phase lock and predominately white phase noise of the interlocked Kerr comb, the auxiliary comb, and the frequency counter with respect to the RF clock [28]. Even though both combs share the same RF clock, they utilize separate electronic frequency synthesizers in their phase-locked loops. The synthesizers' noise contribution [black dashed line in Fig. 4(a)] is currently the limiting factor in our optical synthesis chain. The residual noise added to the optical-comb frequencies by the feedback loops is estimated to be $4 \times 10^{-14}/\tau$ [solid black line in Fig. 4(a)] indicating the potential to utilize much more stable reference oscillators.

A user can take advantage of phase-stabilized frequency combs for synchronization between remote locations, like time transfer and multi-static radar detection. We utilize a ~30-m fiber path between laboratories without active noise cancellation to compare the interlocked Kerr comb and the auxiliary comb, and the combs' relative instability is determined by the microwave electronics involved. Still, the benefit of phase coherence between the combs can be understood through their heterodyne-beat frequency counter lineshapes; Fig. 4(b) presents a progression of histograms obtained by binning one record that indicates an optical-frequency measurement imprecision of only 10 Hz after 10 s of averaging time.

In conclusion, we have explored Kerr-microresonator solitons for f_0 stabilization, bringing optical-frequency metrology at 16 digits of precision to photonic-chip devices. Our work realizes three-optical-cycle, ultrabroad bandwidth soliton pulses that repeat every 1 ps, and we leverage key advantages of Kerr microresonators such as small size, photonic integration, and low power consumption. With enhancements to the photonics packaging, and targeted improvements to the SiN comb line power and SHG technology for f-2f detection, it appears possible to realize a centimeter-scale stabilized frequency comb.

Funding. Defense Advanced Research Projects Agency (DARPA) (DODOS); Air Force Office of Scientific Research (AFOSR) (FA9550-16-1-0016); National Institute of Standards and Technology (NIST); NRC.

Acknowledgment. We thank K. Vahala for the silica resonator, SriCo for the waveguide PPLN, and T. Kippenberg for loan of the auxiliary CW laser. We also acknowledge R. Lutwak, and our DODOS collaborators for helpful comments throughout the experiments.

REFERENCES

1. S. A. Diddams, J. Opt. Soc. Am. B **27**, B51 (2010).
2. M. Kues, C. Reimer, P. Roztocki, L. R. Cortés, S. Sciara, B. Wetzel, Y. Zhang, A. Cino, S. T. Chu, B. E. Little, D. J. Moss, L. Caspani, J. Azaña, and R. Morandotti, Nature **546**, 622 (2017).
3. T. J. Kippenberg, R. Holzwarth, and S. A. Diddams, Science **332**, 555 (2011).
4. F. Ferdous, H. Miao, D. E. Leaird, K. Srinivasan, J. Wang, L. Chen, L. T. Varghese, and A. M. Weiner, Nat. Photonics **5**, 770 (2011).
5. S. B. Papp and S. A. Diddams, Phys. Rev. A **84**, 053833 (2011).
6. D. J. Moss, R. Morandotti, A. L. Gaeta, and M. Lipson, Nat. Photonics **7**, 597 (2013).
7. T. Herr, V. Brasch, J. Jost, C. Wang, N. Kondratiev, M. Gorodetsky, and T. Kippenberg, Nat. Photonics **8**, 145 (2014).
8. S. Coen, H. G. Randle, T. Sylvestre, and M. Erkintalo, Opt. Lett. **38**, 37 (2013).
9. I. S. Grudinin, L. Baumgartel, and N. Yu, Opt. Express **21**, 26929 (2013).
10. X. Yi, Q.-F. Yang, K. Y. Yang, M.-G. Suh, and K. Vahala, Optica **2**, 1078 (2015).
11. S. H. Lee, D. Y. Oh, Q.-F. Yang, B. Shen, H. Wang, K. Y. Yang, Y.-H. Lai, X. Yi, X. Li, and K. Vahala, Nat. Commun. **8**, 1295 (2017).
12. A. A. Savchenkov, V. S. Ilchenko, F. Di Teodoro, P. M. Belden, W. T. Lotshaw, A. B. Matsko, and L. Maleki, Opt. Lett. **40**, 3468 (2015).
13. Q. Li, T. C. Briles, D. A. Westly, T. E. Drake, J. R. Stone, B. R. Ilic, S. A. Diddams, S. B. Papp, and K. Srinivasan, Optica **4**, 193 (2017).
14. M. H. Pfeiffer, C. Herkommer, J. Liu, H. Guo, M. Karpov, E. Lucas, M. Zervas, and T. J. Kippenberg, Optica **4**, 684 (2017).
15. S. B. Papp, K. Beha, P. Del'Haye, F. Quinlan, H. Lee, K. J. Vahala, and S. A. Diddams, Optica **1**, 10 (2014).
16. D. C. Cole, E. S. Lamb, P. Del'Haye, S. A. Diddams, and S. B. Papp, Nat. Photonics **11**, 671 (2017).
17. J. Jost, T. Herr, C. Lecaplain, V. Brasch, M. Pfeiffer, and T. Kippenberg, Optica **2**, 706 (2015).
18. P. Del'Haye, A. Coillet, T. Fortier, K. Beha, D. C. Cole, K. Y. Yang, H. Lee, K. J. Vahala, S. B. Papp, and S. A. Diddams, Nat. Photonics **10**, 516 (2016).
19. E. S. Lamb, D. R. Carlson, D. D. Hickstein, J. R. Stone, S. A. Diddams, and S. B. Papp, Phys. Rev. Appl. **9**, 024030 (2018).
20. V. Brasch, M. Geiselmann, T. Herr, G. Lihachev, M. H. Pfeiffer, M. L. Gorodetsky, and T. J. Kippenberg, Science **351**, 357 (2016).
21. V. Brasch, E. Lucas, J. D. Jost, M. Geiselmann, and T. J. Kippenberg, Light Sci. Appl. **6**, e16202 (2017).
22. D. T. Spencer, T. Drake, T. C. Briles, J. Stone, L. C. Sinclair, C. Fredrick, Q. Li, D. Westly, B. R. Ilic, A. Bluestone, N. Volet, T. Komljenovic, L. Chang, S. H. Lee, D. Y. Oh, M.-G. Suh, K. Y. Yang, M. H. P. Pfeiffer, T. J. Kippenberg, E. Norberg, L. Theogarajan, K. Vahala, N. R. Newbury, K. Srinivasan, J. E. Bowers, S. A. Diddams, and S. B. Papp, Nature **557**, 81 (2018).
23. K. Y. Yang, D. Y. Oh, S. H. Lee, Q.-F. Yang, X. Yi, B. Shen, H. Wang, and K. Vahala, Nat. Photonics **12**, 297 (2018).
24. J. Stone, T. Briles, T. Drake, D. Spencer, D. Carlson, S. Diddams, and S. Papp, arXiv:1708.08405 (2017).
25. T. C. Briles, J. R. Stone, T. E. Drake, D. T. Spencer, S. A. Diddams, and S. B. Papp, in preparation (2017).
26. Y. Okawachi, M. R. Lamont, K. Luke, D. O. Carvalho, M. Yu, M. Lipson, and A. L. Gaeta, Opt. Lett. **39**, 3535 (2014).
27. G. G. Ycas, F. Quinlan, S. A. Diddams, S. Osterman, S. Mahadevan, S. Redman, R. Terrien, L. Ramsey, C. F. Bender, B. Botzer, and S. Sigurdson, Opt. Express **20**, 6631 (2012).
28. T. Dunker, H. Hauglin, and O. P. Rønningen, in *European Frequency and Time Forum (EFTF)* (IEEE, 2016), pp. 1–4.